

Morphometric study of the left atrial appendage related to closure device deployment: a cadaveric study in Thai population

M. Panyawongkhanti, P. Fuktongphan, V. Chentanez

Department of Anatomy, Faculty of Medicine, King Chulalongkorn Memorial Hospital, Chulalongkorn University, Bangkok, Thailand

[Received: 2 April 2019; Accepted: 22 May 2019]

Background: This study aims to investigate the left atrial appendage (LAA) regarding external morphology, positional relation of the ostium of LAA to the left superior pulmonary vein (LSPV), ostium shape, ostium diameter and functional depth.

Materials and methods: Left atrial appendages of 65 cadaveric hearts were examined.

Results: The prevalence of Cauliflower, Windsock, Cactus and Chicken wing type of LAA were 27.7%, 27.7%, 26.1%, and 18.5%, respectively. LAA with two lobes was the most common. All specimens showed no accessory LAA. The relation of the ostium to the LSPV was found in two types which were mid-type (LAA ostium was at the same level as LSPV) in 29 (44.6%) cases and inferior type (LAA ostium was below the level of LSPV) in 36 (55.4%) cases. The shapes of LAA ostium were oval and round with a prevalence of 55.4% and 44.6%, respectively. The diameter of round type ranged from 9.53 to 21.51 mm with a mean of 14.56 ± 2.6 mm. While in oval type, the long and short diameters ranged from 11.61 to 31.71 mm with a mean of 14.23 ± 4.2 mm and from 6.70 to 23.90 mm with a mean of 11.66 ± 3.5 mm, respectively. The surface area of the ostium was calculated from the ostium diameter, range from 71.29 to 594.92 mm² with a mean of 169.56 ± 84.73 mm². There was no statistically significant difference of the surface area between LAA types. The mean functional depth of LAA was 11.57 ± 4.43 mm. The functional depth of the Windsock-type appeared to be statistically significant from the others. However, there was no correlation between the functional depth and the ostium surface area.

Conclusions: This morphometric data might be beneficial for deployment of LAA closure device in the Thai population. (Folia Morphol 2020; 79, 1: 79–85)

Key words: left atrial appendage (LAA), functional depth of LAA, LAA closure, left superior pulmonary vein, ostium diameter, ostium shape, ostium surface area

INTRODUCTION

The prevalence of atrial fibrillation (AF) in Thai elderly aged more than 65 is 1.9% and tends to be higher in older population [15]. AF is known to be a common risk factor for stroke. Thrombus formation

is contributed from three elements which consist of abnormalities of the heart wall, abnormal blood stasis, and blood constituents as described in Virchow's triad [27]. Abnormalities in coagulation and stasis of blood in the left atrium (LA) and left atrial appendage (LAA)

contribute to stroke risk [10]. Despite efficacy of anti-coagulants, many agents used in clinical practice are still not able to prevent thromboembolic stroke due to high cost and lack of reversibility if bleeding occurs. The risks of anticoagulants lead to great interest in alternative treatment including site-specific therapy of LAA occlusion. An LAA closure device acts as an occluder to prevent emboli from LAA to flow into the blood stream which may cause life-threatening embolic events such as embolic ischaemic stroke or myocardial infarction [2].

The Watchman device is the only device that is Food and Drug Administration (FDA) approved [5, 12, 19]. Several parameters such as ostium size and shape, depth of LAA and morphological type of LAA must be determined prior to and during device deployments [19, 28]. Matching of the proper size of the device to LAA morphology is necessary. Complications of the Watchman device deployment usually include peri-procedural pericardial effusion and procedural stroke, which can be reduced by interventionist's experience according to PROTECT-AF trial [16]. Morphological data of LAA is useful for prevention of procedural complication. Investigations of LAA morphological data in both living-patient and in cadaveric specimen were performed in computed tomography (CT)/magnetic resonance imaging (MRI)/echocardiography and cadaveric examination [1, 3, 4, 7–9, 11, 13, 14, 16–18, 20–22, 25, 29]. However, the functional depth of the LAA in each type and its ostium surface area still lacks in cadaveric study [5, 18, 20]. These data are necessary for the matching of appropriate device size to the LAA. Currently, morphometric data of LAA in Thai population are still unavailable. Therefore, the authors conducted this study to provide practical data for deployment of the LAA closure device in Thai population. Morphological details of LAA in cadaveric specimens of non-congenital anomaly heart obtained from the Department of Anatomy, Faculty of Medicine, Chulalongkorn University were investigated.

MATERIALS AND METHODS

Sixty-five formaldehyde-embalmed cadaveric hearts from 23 females and 42 males (age range 30–107) were provided by the Department of Anatomy, Faculty of Medicine, Chulalongkorn University. All specimens had no gross evidence of congenital cardiac anomaly. The LAA was inspected externally for determining morphological type based on Wang's classification (Table 1) and number of LAA lobe was identified and counted in each specimen. The occurrence of accessory LAA which is a common anatomic

Table 1. Main characteristics of left atrial appendage (LAA) type based on Wang's classification [24]

The LAA type	Main characteristics
Chicken wing	An obvious bend in the proximal or middle part of the dominant lobe
Windsock	One dominant lobe of sufficient length as the primary structure
Cauliflower	Limited overall length, more complex internal characteristics and a number of significant lobes present without one dominant lobe
Cactus	A dominant central lobe with secondary lobes extending from the central lobe in both superior and inferior directions

variation of LAA, often arises from the right upper wall of the LA [21] was searched around the atrioventricular region. After external morphology was recorded, the LA wall was incised vertically at 1 cm from the right border paralleled to the right superior and inferior pulmonary veins. Then, horizontal incision was made 0.5 cm above the coronary sulcus. The posterior wall of LA was everted to expose the LAA ostium (Fig. 1). The position of LAA ostium in relation to the left superior pulmonary vein (LSPV) was categorised into superior, mid and inferior type. The shape of the LAA ostium was noted as oval or round and its diameter was determined. In case of oval shape, the long and short perpendicular diameters were measured (Fig. 1A). After the diameter of each type was obtained, surface area of the ostium was calculated using this formula: $A = \pi r_1 r_2$ ($r = \text{Diameter}/2$). In order to prevent the deviation of the spinal needle, a 2 mm in thickness dough pad with a diameter close to the ostium was placed on the ostium and an 18-gauge spinal needle was inserted perpendicularly into the centre of the ostium until its tip touched the LAA wall. Functional depth was determined by measuring the length of the needle from the dough pad to its tip (Fig. 2) by a micrometre in 2 point decimal format. Each parameter was measured twice and the average was calculated. To ensure consistency, the same micrometre was used and all measurements were performed by the same investigator.

Statistical analysis

Statistical analysis was performed by using IBM SPSS Statistics Base version 22.0. Mean and standard deviation of each parameter was obtained. Levene's test was conducted to verify homogeneity of variance. One-way ANOVA was used to compare functional depth and surface area of the ostium between

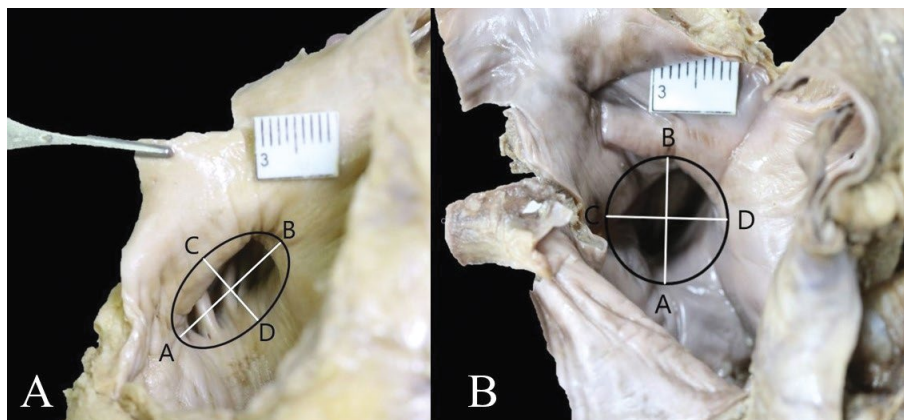


Figure 1. The left atrial wall was everted to evaluate the shape and diameter of left atrial appendage (LAA) ostium; **A.** Oval type ostium, long diameter (AB) and short diameter (CD); **B.** Round type ostium, both diameter (AB and CD) were equal.

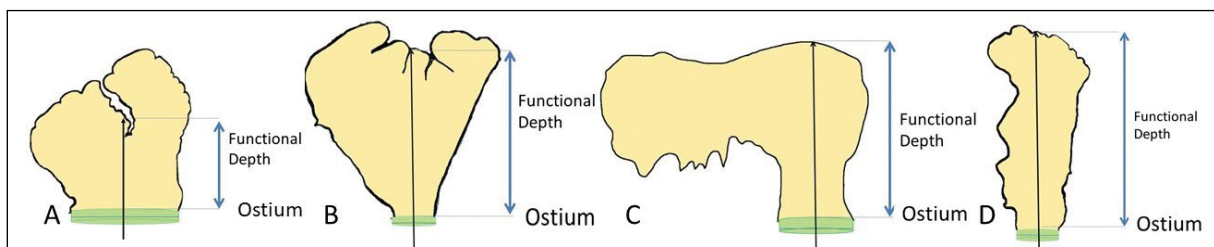


Figure 2. Diagram showing the measurement of functional depth of left atrial appendage (LAA); **A.** Cactus; **B.** Cauliflower; **C.** Chicken wing; **D.** Windsock.

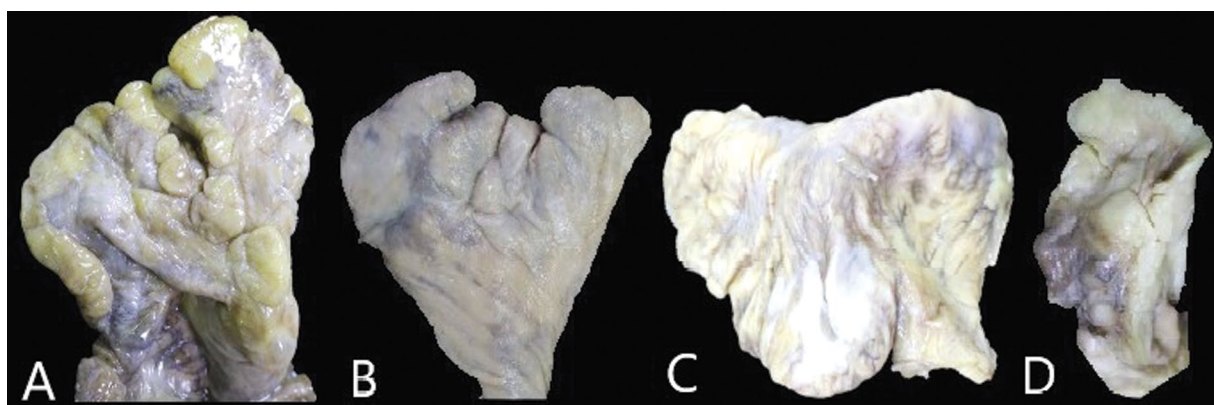


Figure 3. The morphological type of left atrial appendage (LAA) based on Wang’s classification; **A.** Cactus; **B.** Cauliflower; **C.** Chicken wing; **D.** Windsock.

types of LAA. The correlation coefficient was used to measure statistical dependence between functional depth and ostium surface area. A p value < 0.05 was determined as statistically significant.

Ethical consideration

This cadaveric study has been approved by the Institutional Review Board (IRB), Faculty of Medicine, Chulalongkorn University (IRB NO.112/62).

RESULTS

External morphology, types and number of LAA lobe

According to Wang’s classification, the number and percentage of each type was: Cauliflower (18, 27.7%), Windsock (18, 27.7%), Cactus (17, 26.1%) and Chicken wing (12, 18.5%) (Fig. 3). The number of LAA lobe ranged from 1 to 3 lobes. LAA with double lobes was the most common (34, 52.4%), followed by one lobe (22, 33.8%), and three lobes

Table 2. Morphology and morphological data of the left atrial appendage (LAA)

Type of LAA appendage		Cactus	Cauliflower	Chicken wing	Windsock	Total	
N		17	18	12	18	65	
Shape of ostium	Oval	11	9	8	8	36	
	Round	6	9	4	10	29	
Ostium surface area [mm ²]	Mean ± SD (range)	199.13 ± 116.21 (93.20–594.93)	151.08 ± 78.82 (71.29–363.20)	174.98 ± 77.08 (78.93–296.36)	156.50 ± 53.15 (84.27–284.67)	169.56 ± 84.73 (71.29–594.93)	
	95% CI for mean	Upper bound	258.88	190.28	223.95	182.94	190.56
		Lower bound	139.38	111.88	126.01	130.07	148.56
Functional depth [mm]	Mean ± SD (range)	12.71 ± 6.14 (6.54–32.14)	9.86 ± 2.44 (4.87–13.86)	8.99 ± 2.78 (4.48–13.71)	13.94 ± 3.54 (6.65–20.29)	11.57 ± 4.43 (4.48–32.14)	
	95% CI for mean	Upper bound	15.87	11.07	10.76	15.1	12.67
		Lower bound	9.55	8.64	7.22	12.17	10.47

CI — confidence interval; SD — standard deviation

(9, 13.8%), respectively. All samples showed no accessory LAA.

The positional relation to the LSPV, shape, diameter and surface area of the LAA ostium

Results of the positional relation of the LAA ostium to the LSPV showed that no single specimen was superior type. The number and percentage of each positional relation to the LSPV was 29 (44.6%) for the mid-type and 36 (55.4%) for the inferior type.

The shape of the ostium was oval and round. The number and percentage of oval and round types were 36 (55.4%) and 29 (44.6%), respectively. In round type, the diameter ranged from 9.53 to 21.51 mm with a mean of 14.56 ± 2.6 mm. While in oval type, the long diameter ranged from 11.61 to 31.71 mm with a mean of 14.23 ± 4.2 mm, and the short diameter ranged from 6.70 to 23.90 with a mean of 11.66 ± 3.5 mm. Surface areas varied widely ranging from 71.29 to 594.92 mm² with a mean of 169.56 ± 84.73 mm². Details of shape and surface area of the ostium are shown in Table 2. Furthermore, the surface area of the ostium did not show any statistically significant difference in type of LAA.

The functional depth of LAA and its correlation with ostium surface area

Functional depth of LAA ranged from 4.48 to 32.14 mm. The mean of the functional depth of LAA in each type is shown in Table 2. Statistical analysis revealed that the functional depth of Windsock type was statistically significant different from the other types ($p = 0.036$). The correlation coefficient showed

no significant correlation between the surface area of LAA ostium and functional depth of LAA ($r = 0.195$, $p = 0.119$).

DISCUSSION

Nowadays, the LAA is known as the anatomical area responsible for the embolic ischaemic phenomenon in AF patients [2]. Many devices are developed to prevent emboli from LAA. The Watchman's device is the only FDA-approved device [5, 12]. Several parameters such as the ostium size and shape, depth of LAA and morphological type of LAA were used before and during device deployment [28]. There are many reports that have involved the classification of external morphology of LAA, but the most common one is Wang's classification which consists of four types; Chicken wing, Cactus, Cauliflower, and Windsock. In this study population, prevalence of each type was similar to previous studies in CT, MRI and 3-dimensional transoesophageal echocardiography (Table 3) [1, 3, 6–9, 13, 14, 25]. Windsock LAA was reported as the most common type and Chicken wing was the least common type in a previous cadaveric study [20]. In this study, Windsock and Cauliflower were found equally while Chicken wing was found least. Two previous cadaveric studies did not describe the type of LAA [5, 18]. Different results were reported in imaging studies (Table 3). However, the outer shape of appendage does not have to resemble the inner cavity of the LAA, in order to assess the inner cavity appearance of LAA, other method of examine must be proceed such as moulding the cast of LAA. Shape and size of LAA ostium are also factors to consider prior

Table 3. Comparison of morphological types of the left atrial appendage, shape, diameter and surface area of the ostium between this study and eight previous studies

	Wang et al. [24]	Di Biase et al. [1]	Kong et al. [9]	Kimura et al. [8]	Khurram et al. [7]	Nedios et al. [14]	Su et al. [19]	Überler et al. [13]	Current study
Method	CT	CT or MRI	CT	CT	CT	CT	GS	GS	GS
N	612	932	219	80	1063	100	31	56	65
Morphological type									
Chicken wing	18.3%	48%	52.2%	17.5%	45.1%	32%		12%	18%
Windsock	46.7%	19%	23.9%	37.5%	26.4%	10%		38%	28%
Cauliflower	29.1%	3%	13.0%	40%	10.3%	40%		26%	28%
Cactus	5.9%	30%	10.9%	5%	18.4%	18%		24%	26%
Type of ostium									
Oval	68.9%							37.5%	55%
Round	5.7%							62.5	45%
Other	25.4%								
Diameter of ostium [mm] (mean \pm SD)									
Oval shape (long, short diameter)	25.4 \pm 5.5 16.8 \pm 4.5						17.4 \pm 4.0 10.9 \pm 4.2	16.5 \pm 4.0 10.7 \pm 3.9	17.2 \pm 4.2 11.6 \pm 3.5
Round shape	24.6 \pm 4.7								14.5 \pm 2.6
Unspecified type			*25.14 \pm 5.5 24.14 \pm 3.58 26.07 \pm 3.26 27.38 \pm 3.70		27.4 \pm 7.1	**20 \pm 4 18 \pm 4 19 \pm 5 21 \pm 4			
Surface area [mm ²] (mean \pm SD)	374.5 \pm 184.4			462.5 \pm 213.4		**36 \pm 15 45 \pm 28 35 \pm 16 32 \pm 15			169.56 \pm 84.73
Distance from the orifice to the first bend [mm] (mean \pm SD)	14.1 \pm 4.0						7–12 (range)		11.57 \pm 4.43

*, **In order of Chicken wing, Windsock, Cauliflower, and Cactus, respectively; CI — confidence interval; CT — computed tomography; GS — gross specimen; MRI — magnetic resonance imaging; SD — standard deviation

to device deployment and this study revealed that both oval and round shape were found in a similar proportion. The variability of ostium shape was found in many studies [18, 20, 22, 25]. This may be due to the different methods of study in the living or in cadavers (Table 3). Nonetheless, the evaluation of shape and size of ostium by inspecting the cadaveric specimen is rather approximate due to many confounding factors such as the stiffness of the specimen or the measurement's precision etc. Peri-device leakage after Watchman's device deployment was found in 30% of patients and increased in each serial examination [23]. Thus, matching of the appropriate size of the device to the ostium is critical. The diameter of ostium is also a very essential parameter in order to select proper device size to deploy according to the Watchman device implantation overview [24]. The selected

device must achieve 8% to 20% compression [24]. The result of Thai population showed that the maximal diameter of the ostium in oval shape was 17.23 ± 4.20 mm and in round shape was 14.55 ± 2.59 mm which were less than previous studies (Table 3). The surface area of the ostium was also showed in the same way as ostium diameter. These results might be useful to best match the LAA occluding device for Thai patients.

The functional depth of LAA measured in this study was defined as the distance from the ostium surface to the first bend of the LAA. Functional depth of LAA is a crucial factor to prevent the pericardial effusion complication in device deployment. Puncture and breakage to the LAA wall of the device is a severe and commonly occurring complication [16]. Comparing to previous studies, the current study

measured functional depth by using an 18-gauge spinal needle to define the distance from the ostium to the atrial wall of the first bend of LAA, while others measured by imaging modality [4, 17, 25, 29] and cast mould from LAA cadaveric specimens [18]. From this study, there was a range of variations in functional depth according to size and type of LAA. Furthermore, the functional depth of the Windssock type was significantly different when compared to other groups. This result is expected given the shape of the Windssock type which usually bends in less angle and consists of only one dominant lobe. Using the spinal needle to estimate the functional depth may be not representing the actual depth. Its tip can enter far and to very narrow parts of the LAA cavity as shown in Figure 2. In the practice, the pigtail-guide ending is much wider which limits the penetration to the narrow part of the LAA cavity. As aforementioned, the most life-threatening and common peri-procedural complication is pericardial effusion, which is a result from advancing the device too deeply, thereby penetrating the LAA wall. Therefore, the correlation between functional depth and ostium surface area was evaluated and showed no correlation between these two parameters ($r = 0.195$, $p = 0.119$). From the previous study, it was shown that increasing the number of LAA lobes was significantly associated with the existing LAA thrombus despite the clinical risk and blood stasis [26]. Results of the LAA lobe number showed similarity to earlier researches that the maximum number was three lobes, but the prevalence of each number of lobes was not concordant with others [20, 25]. The accessory lobe of LAA which often arises from the right upper wall of the LA was reported in 3 patients in the study of Vargas et al. ($n = 54$) [21]. One of them contained a thrombus. There was no accessory LAA lobe in this current study.

During occluding device deployment, one of the essential landmarks is the LSPV. Therefore, the relationship between LAA ostium and the LSPV was studied and classified by López-Minguez et al. [11] into three types, superior-type (LAA ostium level was above LSPV), mid-type (LAA ostium was at the same level as LSPV) and inferior type (LAA ostium was in at the level below LSPV). The result of this study revealed that only two relations, inferior-type and mid-type were presented. The inferior type was more common. This data was in accordance to the previous cadaveric study which reported that the superior-type was the least common [20].

Limitations of the study

Limitations of this study included the use of embalmed cadavers which might yield different results from fresh or soft-embalmed cadaveric hearts. Also, all specimens were collected from donors with the average age of 60 and we did not know whether or not they were AF patients. Increasing the number of specimens and knowing the history of heart disease may show other significant results. As aforementioned discussed, moulding the cast to evaluate in inner cavity of LAA may yield more accurate parameter.

CONCLUSIONS

The morphology and morphometric data of the LAA in Thai cadaveric specimen was described; the proportion of each morphological category based on Wang's classification was in similar proportion. Two-lobes-LAA is the most common in our samples. Osmium shape of both oval and round type, was also in similar proportion. The surface area of the ostium appeared to have significant variation, but the relationship between surface area and each morphological type was not found. The functional depth of LAA was also varied depending on the morphological type of LAA. Windssock-type functional depth appears to be significantly different from other types. There is no accessory lobe of LAA found in the study samples. The most common relationship between LAA and LPSV found in this study was the inferior-type.

Acknowledgements

The authors would like to thank with sincere appreciation all those who have donated their bodies for medical study and research. Special thanks to Professor Sithiporn Agthong for his kind comments and to the staff of the Department of Anatomy, Faculty of Medicine, Chulalongkorn University for study assistance.

REFERENCES

1. Di Biase L, Santangeli P, Anselmino M, et al. Does the left atrial appendage morphology correlate with the risk of stroke in patients with atrial fibrillation? Results from a multicenter study. *J Am Coll Cardiol.* 2012; 60(6): 531–538, doi: [10.1016/j.jacc.2012.04.032](https://doi.org/10.1016/j.jacc.2012.04.032), indexed in Pubmed: [22858289](https://pubmed.ncbi.nlm.nih.gov/22858289/).
2. Fountain RB, Holmes DR, Chandrasekaran K, et al. The PROTECT AF (WATCHMAN Left Atrial Appendage System for Embolic PROTECTION in Patients with Atrial Fibrillation) trial. *Am Heart J.* 2006; 151(5): 956–961, doi: [10.1016/j.ahj.2006.02.005](https://doi.org/10.1016/j.ahj.2006.02.005), indexed in Pubmed: [16644311](https://pubmed.ncbi.nlm.nih.gov/16644311/).
3. Fukushima K, Fukushima N, Kato K, et al. Correlation between left atrial appendage morphology and flow velocity

- in patients with paroxysmal atrial fibrillation. *Eur Heart J Cardiovasc Imaging*. 2016; 17(1): 59–66, doi: [10.1093/ehjci/jev117](https://doi.org/10.1093/ehjci/jev117), indexed in Pubmed: [25944049](https://pubmed.ncbi.nlm.nih.gov/25944049/).
4. Glassy MS, Sharma G, Singh GD, et al. Usable implantation depth for watchman left atrial appendage occlusion is greater with appendage angiography than transesophageal echocardiography. *Catheter Cardiovasc Interv*. 2019; 93(5): E311–E317, doi: [10.1002/ccd.27916](https://doi.org/10.1002/ccd.27916), indexed in Pubmed: [30311343](https://pubmed.ncbi.nlm.nih.gov/30311343/).
 5. Kamiński R, Kosiński A, Brala M, et al. Variability of the Left Atrial Appendage in Human Hearts. *PLoS One*. 2015; 10(11): e0141901, doi: [10.1371/journal.pone.0141901](https://doi.org/10.1371/journal.pone.0141901), indexed in Pubmed: [26544191](https://pubmed.ncbi.nlm.nih.gov/26544191/).
 6. Khurram IM, Dewire J, Mager M, et al. Relationship between left atrial appendage morphology and stroke in patients with atrial fibrillation. *Heart Rhythm*. 2013; 10(12): 1843–1849, doi: [10.1016/j.hrthm.2013.09.065](https://doi.org/10.1016/j.hrthm.2013.09.065), indexed in Pubmed: [24076444](https://pubmed.ncbi.nlm.nih.gov/24076444/).
 7. Kimura T, Takatsuki S, Inagawa K, et al. Anatomical characteristics of the left atrial appendage in cardiogenic stroke with low CHADS2 scores. *Heart Rhythm*. 2013; 10(6): 921–925, doi: [10.1016/j.hrthm.2013.01.036](https://doi.org/10.1016/j.hrthm.2013.01.036), indexed in Pubmed: [23384894](https://pubmed.ncbi.nlm.nih.gov/23384894/).
 8. Kong B, Liu Yu, Hu He, et al. Left atrial appendage morphology in patients with atrial fibrillation in China: implications for stroke risk assessment from a single center study. *Chin Med J (Engl)*. 2014; 127(24): 4210–4214, indexed in Pubmed: [25533823](https://pubmed.ncbi.nlm.nih.gov/25533823/).
 9. Lee JM, Seo J, Uhm JS, et al. Why is left atrial appendage morphology related to strokes? An analysis of the flow velocity and orifice size of the left atrial appendage. *J Cardiovasc Electrophysiol*. 2015; 26(9): 922–927, doi: [10.1111/jce.12710](https://doi.org/10.1111/jce.12710), indexed in Pubmed: [25959871](https://pubmed.ncbi.nlm.nih.gov/25959871/).
 10. Lip GYH, Lim HS. Atrial fibrillation and stroke prevention. *Lancet Neurol*. 2007; 6(11): 981–993, doi: [10.1016/S1474-4422\(07\)70264-8](https://doi.org/10.1016/S1474-4422(07)70264-8), indexed in Pubmed: [17945152](https://pubmed.ncbi.nlm.nih.gov/17945152/).
 11. López-Mínguez JR, González-Fernández R, Fernández-Vegas C, et al. Anatomical classification of left atrial appendages in specimens applicable to CT imaging techniques for implantation of amplatzer cardiac plug. *J Cardiovasc Electrophysiol*. 2014; 25(9): 976–984, doi: [10.1111/jce.12429](https://doi.org/10.1111/jce.12429), indexed in Pubmed: [24716814](https://pubmed.ncbi.nlm.nih.gov/24716814/).
 12. Moussa Pacha H, Al-Khadra Y, Soud M, et al. Percutaneous devices for left atrial appendage occlusion: a contemporary review. *World J Cardiol*. 2019; 11(2): 57–70, doi: [10.4330/wjc.v11.i2.57](https://doi.org/10.4330/wjc.v11.i2.57), indexed in Pubmed: [30820276](https://pubmed.ncbi.nlm.nih.gov/30820276/).
 13. Nedios S, Koutalas E, Kornej J, et al. Cardiogenic stroke despite low CHA-DS-VASc score: assessing stroke risk by left atrial appendage anatomy (ASK LAA). *J Cardiovasc Electrophysiol*. 2015; 26(9): 915–921, doi: [10.1111/jce.12749](https://doi.org/10.1111/jce.12749), indexed in Pubmed: [26178767](https://pubmed.ncbi.nlm.nih.gov/26178767/).
 14. Petersen M, Roehrich A, Balzer J, et al. Left atrial appendage morphology is closely associated with specific echocardiographic flow pattern in patients with atrial fibrillation. *Europace*. 2015; 17(4): 539–545, doi: [10.1093/europace/euu347](https://doi.org/10.1093/europace/euu347), indexed in Pubmed: [25491111](https://pubmed.ncbi.nlm.nih.gov/25491111/).
 15. Phrommintikul A, Detnuntarat P, Prasertwitayakij N, et al. Prevalence of atrial fibrillation in Thai elderly. *J Geriatr Cardiol*. 2016; 13(3): 270–273, doi: [10.11909/j.issn.1671-5411.2016.03.002](https://doi.org/10.11909/j.issn.1671-5411.2016.03.002), indexed in Pubmed: [27103924](https://pubmed.ncbi.nlm.nih.gov/27103924/).
 16. Reddy VY, Holmes D, Doshi SK, et al. Safety of percutaneous left atrial appendage closure: results from the watchman left atrial appendage system for embolic protection in patients with AF (PROTECT AF) clinical trial and the continued access registry. *Circulation*. 2011; 123(4): 417–424, doi: [10.1161/CIRCULATIONAHA.110.976449](https://doi.org/10.1161/CIRCULATIONAHA.110.976449), indexed in Pubmed: [21242484](https://pubmed.ncbi.nlm.nih.gov/21242484/).
 17. Song H, Zhou Q, Zhang L, et al. Evaluating the morphology of the left atrial appendage by a transesophageal echocardiographic 3-dimensional printed model. *Medicine (Baltimore)*. 2017; 96(38): e7865, doi: [10.1097/MD.00000000000007865](https://doi.org/10.1097/MD.00000000000007865), indexed in Pubmed: [28930824](https://pubmed.ncbi.nlm.nih.gov/28930824/).
 18. Su P, McCarthy KP, Ho SY. Occluding the left atrial appendage: anatomical considerations. *Heart*. 2008; 94(9): 1166–1170, doi: [10.1136/hrt.2006.111989](https://doi.org/10.1136/hrt.2006.111989), indexed in Pubmed: [17488765](https://pubmed.ncbi.nlm.nih.gov/17488765/).
 19. Suradi HS, Hijazi ZM. Left atrial appendage closure: outcomes and challenges. *Neth Heart J*. 2017; 25(2): 143–151, doi: [10.1007/s12471-016-0929-0](https://doi.org/10.1007/s12471-016-0929-0), indexed in Pubmed: [27943175](https://pubmed.ncbi.nlm.nih.gov/27943175/).
 20. Üçerler H, İkiz ZA, Özgür T. Human left atrial appendage anatomy and overview of its clinical significance. *Anadolu Kardiyol Derg*. 2013; 13(6): 566–572, doi: [10.5152/akd.2013.181](https://doi.org/10.5152/akd.2013.181), indexed in Pubmed: [23886901](https://pubmed.ncbi.nlm.nih.gov/23886901/).
 21. Vargas-Barrón J, Espinola-Zavaleta N, Roldán FJ, et al. Transesophageal echocardiographic diagnosis of thrombus in accessory lobes of the left atrial appendage. *Echocardiography*. 2000; 17(7): 689–691, doi: [10.1046/j.1540-8175.2000.00689.x](https://doi.org/10.1046/j.1540-8175.2000.00689.x), indexed in Pubmed: [11107207](https://pubmed.ncbi.nlm.nih.gov/11107207/).
 22. Veinot JP, Harrity PJ, Gentile F, et al. Anatomy of the normal left atrial appendage: a quantitative study of age-related changes in 500 autopsy hearts: implications for echocardiographic examination. *Circulation*. 1997; 96(9): 3112–3115, doi: [10.1161/01.cir.96.9.3112](https://doi.org/10.1161/01.cir.96.9.3112), indexed in Pubmed: [9386182](https://pubmed.ncbi.nlm.nih.gov/9386182/).
 23. Viles-Gonzalez JF, Kar S, Douglas P, et al. The clinical impact of incomplete left atrial appendage closure with the Watchman Device in patients with atrial fibrillation: a PROTECT AF (Percutaneous Closure of the Left Atrial Appendage Versus Warfarin Therapy for Prevention of Stroke in Patients With Atrial Fibrillation) substudy. *J Am Coll Cardiol*. 2012; 59(10): 923–929, doi: [10.1016/j.jacc.2011.11.028](https://doi.org/10.1016/j.jacc.2011.11.028), indexed in Pubmed: [22381428](https://pubmed.ncbi.nlm.nih.gov/22381428/).
 24. Waksman R, Pendyala LK. Overview of the Food and Drug Administration circulatory system devices panel meetings on WATCHMAN left atrial appendage closure therapy. *Am J Cardiol*. 2015; 115(3): 378–384, doi: [10.1016/j.amjcard.2014.11.011](https://doi.org/10.1016/j.amjcard.2014.11.011), indexed in Pubmed: [25579887](https://pubmed.ncbi.nlm.nih.gov/25579887/).
 25. Wang Y, Di Biase L, Horton RP, et al. Left atrial appendage studied by computed tomography to help planning for appendage closure device placement. *J Cardiovasc Electrophysiol*. 2010; 21(9): 973–982, doi: [10.1111/j.1540-8167.2010.01814.x](https://doi.org/10.1111/j.1540-8167.2010.01814.x), indexed in Pubmed: [20550614](https://pubmed.ncbi.nlm.nih.gov/20550614/).
 26. Yamamoto M, Seo Y, Kawamatsu N, et al. Complex left atrial appendage morphology and left atrial appendage thrombus formation in patients with atrial fibrillation. *Circ Cardiovasc Imaging*. 2014; 7(2): 337–343, doi: [10.1161/CIRCIMAGING.113.001317](https://doi.org/10.1161/CIRCIMAGING.113.001317), indexed in Pubmed: [24523417](https://pubmed.ncbi.nlm.nih.gov/24523417/).
 27. Yamashita T. Virchow triad and beyond in atrial fibrillation. *Heart Rhythm*. 2016; 13(12): 2377–2378, doi: [10.1016/j.hrthm.2016.09.007](https://doi.org/10.1016/j.hrthm.2016.09.007), indexed in Pubmed: [27616698](https://pubmed.ncbi.nlm.nih.gov/27616698/).
 28. Yeow WL, Kar S. Device- and laa-specific characteristics for successful LAA closure: tips and tricks. *Interv Cardiol Clin*. 2014; 3(2): 239–254, doi: [10.1016/j.iccl.2013.12.002](https://doi.org/10.1016/j.iccl.2013.12.002), indexed in Pubmed: [28582169](https://pubmed.ncbi.nlm.nih.gov/28582169/).
 29. Zhang J, Cui CY, Huang DQ, et al. Evaluation of the left atrial appendage by real time three-dimensional transesophageal echocardiography online. *Echocardiography*. 2018; 35(7): 991–998, doi: [10.1111/echo.13870](https://doi.org/10.1111/echo.13870), indexed in Pubmed: [29676485](https://pubmed.ncbi.nlm.nih.gov/29676485/).